Nanograin nucleation initiated by intergrain sliding and/or lattice slip in nanomaterials

S. V. Bobylev and I. A. Ovid'ko[a)]
Institute of Problems of Mechanical Engineering, Russian Academy of Sciences, Bolshoj 61, Vasilievskii Ostrov, St. Petersburg 199178, Russia

(Received 27 December 2007; accepted 1 February 2008; published online 27 February 2008)

Stress-induced nucleation of nanoscale grains (nanograins) in deformed nanocrystalline metals and ceramics is theoretically described as a process initiated by intergrain sliding and/or lattice slip. The nanograin nucleation occurs through splitting and migration of grain boundaries containing disclination dipoles produced by intergrain sliding and/or lattice slip. It is shown that the nanograin nucleation is energetically favorable in mechanically loaded nanocrystalline Al and α-Al_2O_3 in certain ranges of their parameters and the external stress level. © *2008 American Institute of Physics*. [DOI: 10.1063/1.2885069]

Nanocrystalline metals and ceramics, hereinafter called nanomaterials, in the course of plastic deformation often show the outstanding mechanical characteristics (superior strength, etc.) attributed to the effects of the nanocrystalline structure; see, e.g., Refs. 1–4. In particular, in parallel with conventional lattice dislocation slip, intergrain sliding and other interface-conducted and -controlled mechanisms of plastic flow are treated to effectively operate in nanomaterials due to their nanocrystallinity.[1–14] On the other hand, the nanocrystalline structure can be formed in initially coarse-grained materials due to deformation processes causing grain refinement.[3,4,15,16] Deformation-induced nanocrystallization is commonly treated to occur through continuous dislocation ensemble evolution resulting in consequent formation of dislocation subboundaries cells and high-angle grain boundaries.[3,4,15,16] Recently, however, computer simulations[17–19] have shown that nanograin nucleation occurs through splitting and migration of grain boundaries (GBs) near their triple junctions in nanomaterials (with metallic and covalent interatomic bonds) during plastic deformation. The micromechanism and driving forces of the nanograin nucleation reported in Refs. 17–19 are unclear. The main aim of this paper is to suggest a theoretical model describing the nanograin nucleation in question as a special deformation mode initiated by intergrain sliding and/or lattice slip.

Let us consider typical defect structures formed at GBs due to lattice dislocation slip and/or intergrain sliding in deformed nanomaterials. The lattice slip in a grain interior "supplies" lattice dislocations to a GB [Fig. 1(a)]. The dislocations in the GB are spread into GB dislocations forming a wall-like configuration [Fig. 1(b)]. As a corollary, tilt misorientation of the GB, after absorption of several dislocations with the same Burgers vectors, changes, say, by value of ω_0, and triple junctions adjacent to the GB become uncompensated [Fig. 1(b)]. In this case, the sums of tilt misorientation angles at the junctions A and B become equal to ω_0 and $-\omega_0$, respectively. In the theory of defects in solids, these junctions are wedge disclinations characterized by the disclination strength $\pm\omega_0$.[20] The disclinations form a dipole configuration [Fig. 1(b)].

Also, GB disclination dipoles typically form in nanomaterials and polycrystals due to intergrain sliding (that dominates, in particular, in superplastic deformation[1,2,4]). Following Ref. 14, intergrain sliding across a triple junction of GBs produces a disclination dipole at a GB fragment along which the triple junction shifts [Figs. 1(d) and 1(e)]. In short, intergrain sliding along the horizontal GB results in the displacement of both the triple junction (from position A to position B) and the vertical GB assumed to be a symmetric tilt boundary with tilt misorientation ω_0. When the triple junction is shifted by intergrain sliding from its initial position A to position B [Fig. 1(e)], the angle gaps ω_0 and $-\omega_0$ appear at triple junction (point) A and double junction (point) B at the

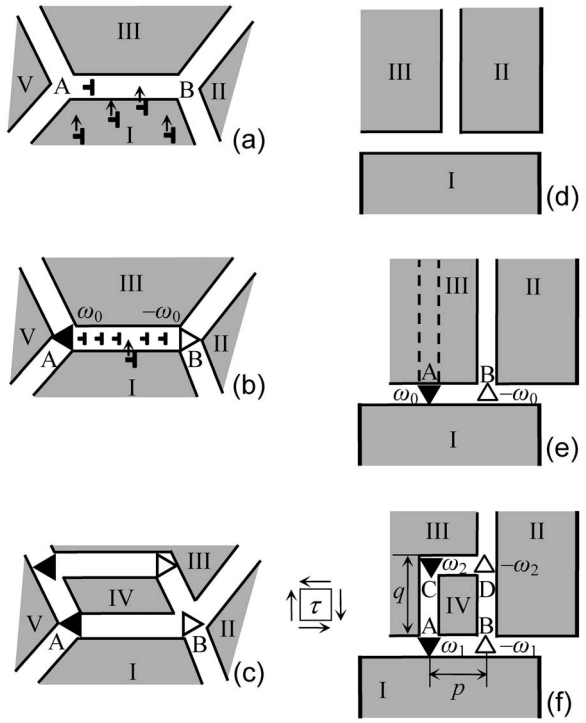

FIG. 1. Defect structure transformations resulting in nanograin nucleation. Formation of a disclination dipole at a grain boundary in a deformed nanomaterial due to [(a) and (b)] lattice dislocation slip causing "bombardment" of the grain boundary by lattice dislocations. [(d) and (e)] Grain boundary sliding and associated movement of triple junction. [(c) and (f)] Processes of nanograin nucleation through splitting and migration of grain boundaries.

[a)]Electronic mail: ovidko@def.ipme.ru.

horizontal GB, respectively.[14] Points A and B are considered as wedge disclinations with the strengths $\pm\omega_0$.[20] They form a dipole [Fig. 1(e)].

GB disclination dipoles under applied stress tend to move causing rotational deformation.[20,21] Also, GB disclinations tend to split because the splitting is driven by decrease of their elastic energy.[20,22] Combining these processes, one finds that GB disclinations can move and split causing nucleation of a nanograin (nanograin IV), as shown in Figs. 1(c) and 1(f). For definiteness, we consider evolution of the disclination dipole shown in Figs. 1(e) and 1(f). The distance between the disclinations of the initial dipole [Fig. 1(e)] is p. Within our model, the nanograin IV nucleates through splitting of the GB AB into the immobile GB AB and the mobile GB CD [Fig. 1(f)]. In general, the splitting of the GB is accompanied by the splitting of the initial dipole of GB disclinations with strengths ω_0 and $-\omega_0$ [located at points A and B, respectively; see Fig. 1(e)] into two dipoles: the immobile dipole of GB disclinations with strengths ω_1 and $-\omega_1$ (located at points A and B, respectively) and the mobile dipole of GB disclinations with strengths ω_2 and $-\omega_2$ (located at points C and D, respectively), see Fig. 1(f). For definiteness, we choose misorientations of GBs generated due the nanograin nucleation [Fig. 1(f)] as those providing the disclination strength conservation law during the splitting: $\omega_0=\omega_1+\omega_2$. The disclination dipole CD moves over distance q in grain III. The crystal lattice in area ABCD swept by the moving GB CD is misoriented relative to lattices in grains I, II, and III [Fig. 1(f)]. In this case, the area ABCD represents the nanograin IV whose formation is associated with movement of disclination dipole CD that carries plastic deformation. As a corollary, the nanograin formation [Fig. 1(f)] serves as a special deformation mode in nanomaterials and polycrystals.

Let us calculate the energy change ΔW [per unit length of a line perpendicular to Fig. 1(f)] that characterizes the nanograin formation [Fig. 1(f)]. The change ΔW contains the six terms:

$$\Delta W = W_{\mathrm{el}}^{\omega_1} + W_{\mathrm{el}}^{\omega_2} - W_{\mathrm{el}}^{\omega_0} + W_{\mathrm{int}} - A + \Delta W_{\mathrm{gb}}. \quad (1)$$

Here, $W_{\mathrm{el}}^{\omega_0}$, $W_{\mathrm{el}}^{\omega_1}$, and $W_{\mathrm{el}}^{\omega_2}$ are the proper elastic energies of dipole of wedge disclinations with strengths $\pm\omega_0$, $\pm\omega_1$, $\pm\omega_2$, respectively, W_{int} is the energy that characterizes the interaction between the disclination dipoles with strengths $\pm\omega_1$ and $\pm\omega_2$, A is the work spent by the external shear stress τ to movement of the ω_2 dipole, ΔW_{gb} is the change in the GB energy due to GB splitting that accompanies nucleation of the grain IV.

The energy change ΔW_{gb} [per unit length of a line perpendicular to Fig. 1(f)] is estimated as

$$\Delta W_{\mathrm{gb}} = \gamma_{\mathrm{gb}}(p+q). \quad (2)$$

Here, γ_{gb} is the specific energy of a tilt GB per unit of its area. In most materials, the GB energy γ versus tilt misorientation θ, for $\theta>15°$, is a slowly increasing or approximately constant function of θ (with energy "cusps" associated with special GBs in some narrow intervals of θ).[23] For simplicity, we do not consider special GBs and assume $\gamma_{\mathrm{gb}}(\theta)$ to be constant. Other five terms on the right-hand side of formula (1) are calculated by standard methods[20] of the theory of disclinations in solids. In doing so, we find the following expression for the energy change ΔW:

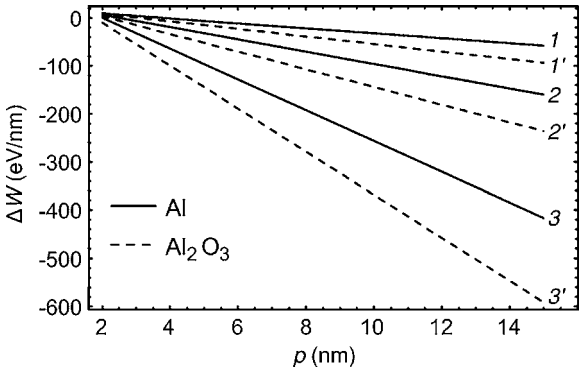

FIG. 2. The dependence of the energy difference ΔW on the distance q moved by grain boundary CD in Al (see solid curves), for $\omega_0=0.6$ and $\tau=0.4$ GPa; Al_2O_3 (see dashed curves), for $\omega_0=0.3$ and $\tau=1.2$ GPa. Curves 1, 2, and 3 (as well as 1′, 2′, and 3′) correspond to the disclination dipole size $p=3$, 5, and 10 nm, respectively.

$$\Delta W = \frac{D\omega_1\omega_2}{2}\left(p^2 \ln\frac{p^2}{p^2+q^2} + q^2 \ln\frac{q^2}{p^2+q^2}\right) - \tau\omega_2 pq + \Delta W_{\mathrm{gb}}, \quad (3)$$

where $D=G/[2\pi(1-\nu)]$, G is the shear modulus, and ν is the Poisson ratio.

With formulas (2) and (3), we calculated the total energy change ΔW in nanocrystalline Al and nanoceramic α-Al_2O_3. In the calculations, we used the following typical values of parameters: for Al,[24] $G=26.5$ GPa and $\nu=0.34$; for α-Al_2O_3,[25] $G=169$ GPa and $\nu=0.23$. Also, for definiteness, the disclination strengths are assumed to obey equations $\omega_1=0$ and $\omega_2=\omega_0$. The grain size (playing role of the upper limit of q and p) is taken as $d=15$ nm. Following experimental data,[26,27] the specific energy of the [110] tilt boundaries with $\theta>15°$ in Al is around $\gamma_{\mathrm{gb}}=0.4\ \mathrm{J/m^2}$. In the experiment,[28] energies of high-angle tilt boundaries with $\theta>15°$ in a α-Al_2O_3 bicrystal with the [0001] rotation axis were measured and found to be in the range from 0.4 to 0.7 $\mathrm{J/m^2}$. For definiteness, in our calculations of ΔW in α-Al_2O_3, we used value of $\gamma_{\mathrm{gb}}=0.5\ \mathrm{J/m^2}$. Figure 2 shows $\Delta W(q)$ in the case of Al (see solid curves), for $\omega_0=0.6$, $\tau=0.4$ GPa, and $p=3$, 5, and 10 nm (see curves 1, 2, and 3, respectively). Dashed curves in Fig. 2 shows $\Delta W(q)$ in the case of α-Al_2O_3, for $\omega_0=0.3$, $\tau=1.2$ GPa, and $p=3$, 5, and 10 nm (see curves 1′, 2′, and 3′, respectively).

Note that the atomistic details of the GB splitting dominate at its very initial stage, for $q<2$ nm. To describe such details, atomistic simulations are needed which are beyond the scope of our continuum approach. At the same time, the energy profit of the GB splitting [Figs. 1(e) and 1(f)] in the range of $q\geqslant 2$ nm is critical for the splitting to occur, because the very initial stage ($q<2$ nm) may occur through thermally assisted formation of steps at the initial GB, if the splitting of the GB at $q\geqslant 2$ nm is energetically favorable. In this context, we will focus our analysis to the situation where $p,q\geqslant 2$ nm. In this situation, the nucleation of the grain IV [Fig. 1(f)] is characterized by the absence of any energy barrier, if the following inequalities are valid:

$$\Delta W(q=2\ \mathrm{nm}) \leqslant 0, \qquad \left.\frac{\partial(\Delta W)}{\partial q}\right|_{q=2\ \mathrm{nm}} \leqslant 0. \quad (4)$$

In terms of the applied stresses, the non-barrier nucleation of the grain IV [Fig. 1(f)] occurs, if the applied shear

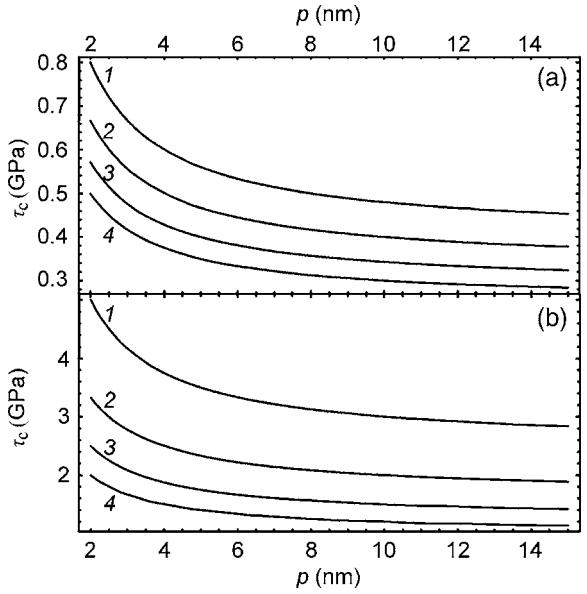

FIG. 3. The dependence of the critical shear stress τ_c on the size p of the disclination dipole AB in (a) Al (curves 1, 2, 3, and 4 correspond to the disclination strength $\omega_0=0.5$, 0.6, 0.7, and 0.8, respectively) and (b) Al_2O_3 (curves 1, 2, 3, and 4 correspond to the disclination strength $\omega_0=0.1$, 0.15, 0.2, and 0.25, respectively).

stress reaches its critical value τ_c. The latter is defined as the minimum stress at which both inequalities (4) are valid. With formulas (2)–(4), after some algebra, we find the following expression for τ_c in realistic ranges of parameters of nanocrystalline Al and Al_2O_3:

$$\tau_c = \left[\frac{D\omega_1}{2} \left(\frac{p}{q} \ln \frac{p^2}{p^2+q^2} + \frac{q}{p} \ln \frac{q^2}{p^2+q^2} \right) + \frac{\gamma_{gb}(p+q)}{\omega_2 pq} \right]_{q=2\ \mathrm{nm}}. \quad (5)$$

When the initial disclination dipole moves without its splitting ($\omega_1=0$ and $\omega_2=\omega_0$), formula (5) for the critical stress τ_c causing the nonbarrier grain nucleation is reduced to the expression:

$$\tau_c = \left. \frac{\gamma_{gb}(p+q)}{\omega_0 pq} \right|_{q=2\ \mathrm{nm}}. \quad (6)$$

Figures 3(a) and 3(b) present the dependence of τ_c on p, calculated by formula (6), in the cases of Al and α-Al_2O_3, respectively. For Al, curves 1, 2, 3, and 4 correspond to values of $\omega_0=0.5$, 0.6, 0.7, and 0.8, respectively [Fig. 3(a)]. These curves show that, for $\omega_0 \geqslant 0.6$, the critical shear stress τ_c is around or lower than the stress $\tau \approx 0.3$ GPa close to real stress values[29] reached in nanocrystalline Al. For α-Al_2O_3, curves 1, 2, 3, and 4 correspond to values of $\omega_0=0.1$, 0.15, 0.2, and 0.25, respectively. These curves show that, for $\omega_0 \geqslant 0.15$, the stress τ_c is around or lower than the shear stress $\tau \approx 3.5$ GPa that can be reached in real nanocrystalline α-Al_2O_3. Following our estimates (Fig. 3), the stress level needed to initiate the nanograin nucleation is rather high. This level is typical for nanomaterials, but, in most cases, exceeds the stresses operating in deformed polycrystals. In this context, though the disclination mode for grain nucleation (Fig. 1) can operate in both nanomaterials and polycrystals, the mode is expected to occur more frequently in nanomaterials, compared to polycrystals.

In summary, we have theoretically described stress-induced nucleation of nanograins in deformed nanomaterials as a process initiated by intergrain sliding and/or lattice slip. It has been shown that the stress-induced nucleation of nanograins occurs in the energy nonbarrier way in nanocrystalline Al and α-Al_2O_3 in certain ranges of their parameters and the applied stress level. Our model accounts for results of computer simulations[17–19] and experiments[30,31] showing grain nucleation at triple junctions of GBs in deformed nanomaterials and polycrystals.

This work was supported, in part, by the Office of U.S. Naval Research (Grant No. N00014-07-1-0295), the Russian Federal Agency of Science and Innovations (Contract No. 02.513.11.3190), the National Science Foundation (grant No. CMMI #0700272), and Russian Academy of Sciences Program "Structural Mechanics of Materials and Construction Elements."

[1] D. Wolf, V. Yamakov, S. R. Phillpot, A. K. Mukherjee, and H. Gleiter, Acta Mater. **53**, 1 (2005).
[2] M. Dao, L. Lu, R. J. Asaro, J. T. M. De Hosson, and E. Ma, Acta Mater. **55**, 4041 (2007).
[3] C. C. Koch, J. Mater. Sci. **42**, 1403 (2007).
[4] C. C. Koch, I. A. Ovid'ko, S. Seal, and S. Veprek, *Structural Nanocrystalline Materials: Fundamentals and Applications* (Cambridge University Press, Cambridge, 2007).
[5] Y. M. Wang and E. Ma, Appl. Phys. Lett. **83**, 3165 (2003); **85**, 2750 (2004).
[6] M. Chen, E. Ma, K. J. Hemker, H. Sheng, Y. Wang, and X. Cheng, Science **300**, 1275 (2003).
[7] X. Z. Liao, F. Zhou, E. J. Lavernia, D. W. He, and Y. T. Zhu, Appl. Phys. Lett. **83**, 5062 (2003).
[8] Y. T. Zhu, X. R. Liao, and R. Z. Valiev, Appl. Phys. Lett. **86**, 103112 (2005).
[9] Y. M. Wang, A. M. Hodge, J. Biener, A. V. Hamza, D. E. Barnes, K. Liu, and T. G. Nieh, Appl. Phys. Lett. **86**, 101915 (2005).
[10] M. Yu. Gutkin and I. A. Ovid'ko, Appl. Phys. Lett. **87**, 251916 (2005).
[11] Y. H. Zhao, Y. T. Zhu, X. R. Liao, Z. Horita, and T. G. Langdon, Appl. Phys. Lett. **89**, 121906 (2006).
[12] X. L. Wu and Y. T. Zhu, Appl. Phys. Lett. **89**, 031922 (2006).
[13] Y. Mo and I. Szlufarska, Appl. Phys. Lett. **90**, 181926 (2007).
[14] I. A. Ovid'ko and A. G. Sheinerman, Appl. Phys. Lett. **90**, 171927 (2007).
[15] H. J. Fecht, E. Hellstern, Z. Fu, and W. L. Johnson, Metall. Trans. A **21**, 2333 (1990).
[16] C. C. Koch, Rev. Adv. Mater. Sci. **5**, 91 (2003).
[17] V. Yamakov, D. Wolf, S. R. Phillpot, A. K. Mukherjee, and H. Gleiter, Nat. Mater. **1**, 45 (2002).
[18] M. J. Demkowicz, A. S. Argon, D. Farkas, and M. Frary, Philos. Mag. **87**, 4253 (2007).
[19] A. Cao and Y. Wei, Phys. Rev. B **76**, 024113 (2007).
[20] A. E. Romanov and V. I. Vladimirov, in *Dislocations in Solids*, edited by F. R. N. Nabarro (North Holland, Amsterdam, 1992), Vol. 9, p. 191.
[21] I. A. Ovid'ko, Science **295**, 2386 (2002).
[22] M. Yu. Gutkin and I. A. Ovid'ko, *Plastic Deformation in Nanocrystalline Materials* (Springer, Berlin, 2004).
[23] A. P. Sutton and R. W. Balluffi, *Interfaces in Crystalline Materials* (Clarendon, Oxford, 1995).
[24] J. P. Hirth and J. Lothe, *Theory of Dislocations* (Wiley, New York, 1982).
[25] R. G. Munro, J. Am. Chem. Soc. **80**, 1919 (1997).
[26] A. Otsuki and M. Mizuno, *Grain Boundary Structure and Related Phenomena*, Supplementary Transactions of JIM Vol. 27 (Japan Institute of Metals, Sendai, 1986), p. 789.
[27] G. C. Hasson and C. Goux, Scr. Metall. **5**, 889 (1971).
[28] T. Watanabe, H. Yoshida, T. Saito, T. Yamamoto, Y. Ikuhara, and T. Sakuma, Mater. Sci. Forum **304-306**, 601 (1999).
[29] W. Xu, T. Honma, and X. Wu, Appl. Phys. Lett. **91**, 031901 (2007).
[30] H. Miura, T. Sakai, H. Hamaji, and J. J. Jonas, Scr. Mater. **50**, 65 (2004).
[31] H. Miura, T. Sakai, S. Andriawanto, and J. J. Jonas, Philos. Mag. **85**, 2653 (2005).